Optics Communications 95 (1993) 97–102
North-Holland

OPTICS
COMMUNICATIONS

Linewidth effects in resonant CARS processes

Ilse Aben, Wim Ubachs, Gert van der Zwan and Wim Hogervorst
Laser Centre, Free University Amsterdam, De Boelelaan 1081, 1081 HV Amsterdam, Netherlands

Received 13 August 1992

The effects of pump-laser bandwidth on spectral linewidth in three different resonant coherent anti-Stokes Raman spectroscopy (CARS) processes in molecular iodine is studied. In only one of the three resonant CARS processes an increase in bandwidth of the pump laser is reflected in a broadening of the spectral features. An investigation of the effects of laser bandwidth therefore may serve to distinguish between different types of four-wave-mixing processes.

1. Introduction

In a recent study [1] three different resonance-enhanced CARS processes $\omega_{AS}=2\omega_1-\omega_2$ were identified in I_2 (ω_1: frequency pump-laser, ω_2: Stokes frequency, ω_{AS}: generated anti-Stokes frequency). Apart from the process with a coherence between rovibrational states in the $X\,^1\Sigma_g^+$ electronic ground state (referred to as ground-state resonant CARS) [2–4], two different types of excited-state CARS processes were observed: excited-state parametric as well as non-parametric CARS. The identification of these threefold resonant four-wave mixing processes was confirmed in two different ways. Firstly, the frequency positions of the spectral features compared very well with calculations based on the accurately known term energies [5] of the $B\,^3\Pi_{u0}^+ - X\,^1\Sigma_g^+$ system of I_2. Secondly, measurements of polarization dependent linestrengths for the excited-state CARS processes confirmed the postulated resonance schemes [6].

In the present work a third confirmation is presented that gives additional support for the correct identification of the different resonance-enhanced CARS processes. The effect of the bandwidth of the pump laser on the spectral linewidth as well as on the frequency position of the CARS-resonances is investigated. A Nd:YAG laser equipped with injection seeder may be used to set the bandwidth of the pump frequency either at 0.005 cm^{-1} (narrowband) or approximately 1 cm^{-1} (broadband). The effect on the width of resolved spectral features is found to depend on the selected CARS-process. The interpretation is consistent with the earlier [1] identification of the resonant CARS processes.

2. General considerations

Four-wave-mixing processes, of which resonant CARS processes are a special subclass, are governed by the third-order nonlinear susceptibility $\chi^{(3)}$. For a qualitative understanding of linewidth effects a consideration of energy level diagram may be elucidating and that is the viewpoint we will take. For explicit expressions of $\chi^{(3)}$ describing the various CARS processes, their relation to energy level diagrams and more details on the characterization of the multiple-resonant CARS processes in I_2 we refer to Aben et al. [1]. In fig. 1 energy-level schemes for the three processes considered, ground-state resonance CARS, excited-state parametric CARS and excited-state non-parametric CARS, are shown. All three processes have in common resonance enhancement by two bound–bound transitions and by a continuum transition; therefore they are called discrete–continuum resonant CARS processes.

The energy level schemes of fig. 1 illustrate that in all three processes the pump frequency ω_1 may be in resonance with an electronic transition when probing a certain ground state $|a\rangle$, $|a'\rangle$ or $|a''\rangle$. To identify the specific quantum states of I_2 that match

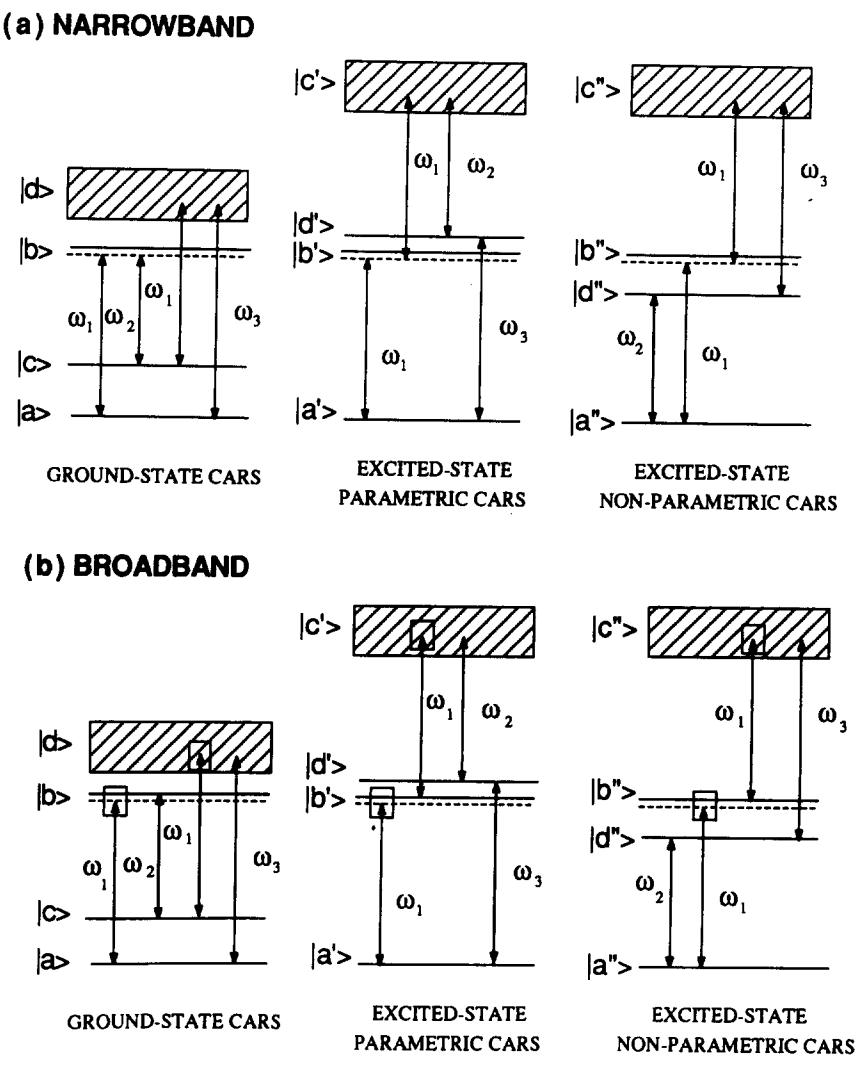

Fig. 1. Energy level schemes for ground-state CARS, excited-state parametric and non-parametric CARS. The shaded area corresponds to a continuum state. (a) Bandwidth of the ω_1-laser < 0.005 cm^{-1}. The dashed lines indicate the energy of the ω_1-photon. (b) Bandwidth of the ω_1-laser ≈ 1 cm^{-1}. This bandwidth is indicated with a rectangle.

this resonance the transition frequencies in the $B\,^3\Pi_{u0}^+ - X\,^1\Sigma_g^+$-system were calculated with the molecular constants of Luc [5]. It was found that for $\omega_1 = 18788.39$ cm^{-1} (centre frequency of the second harmonic of the Nd:YAG laser) resonances may occur for $B\,^3\Pi_{u0}^+$, $v \geqslant 32$. Transitions in the P and R branches in the B–X system for several vibrational states v are plotted in fig. 2 in terms of a detuning from this particular ω_1. This figure shows that the P(53) and R(56) lines of the B–X (32, 0) band and the P(103) line of the B–X (34, 0) band are in resonance with the broadband pump laser; the grey shaded area represents its bandwidth (see section 3.2). The P(83) line of the B–X (33, 0) band is in near-resonance with the broadband laser. The frequency of the narrowband pump (ω_1) may differ from day-to-day as a result of changes in the temperature in the laboratory. The detunings from the one-photon resonances in this case depend on the actual value of ω_1 but are in any case small for the P(53), R(56) and P(103) lines.

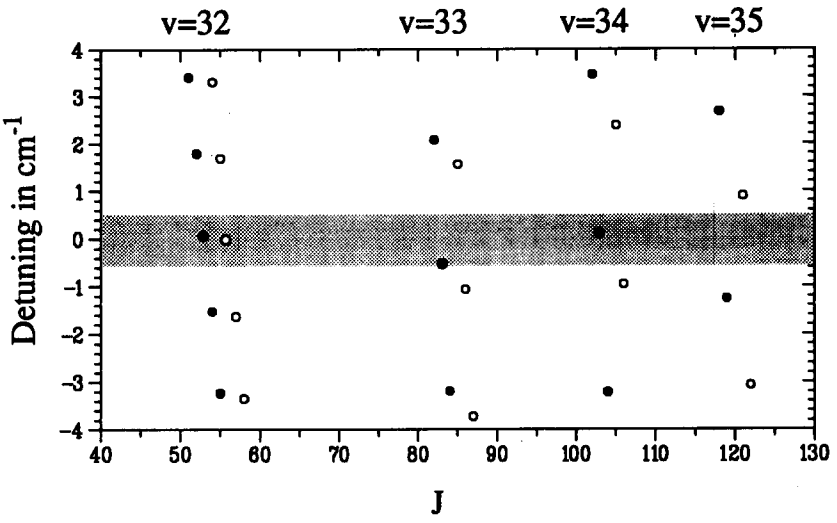

Fig. 2. Frequency-profile of the broadband ω_1 laser in relation to the one-photon resonances in I_2. Black and open circles correspond to P and R transitions in the B–X $(v, 0)$ band, respectively. Zero detuning is at $\omega_1 = 18788.39$ cm^{-1}. This is the experimentally determined centre frequency of the unseeded Nd:YAG laser.

3. Measurements and interpretation

A standard colinear CARS setup is used with an injection-seeded, frequency-doubled Nd:YAG laser at 532 nm as the pump laser (ω_1) and a pulsed dye laser with a bandwidth of 0.07 cm^{-1} providing the tunable Stokes beam (ω_2). When properly seeded the pulsed Nd:YAG laser has a bandwidth close to the Fourier transform limit, so $\Delta\omega_1 < 0.005$ cm^{-1}. The bandwidth of the unseeded pump laser is approximately 1 cm^{-1}.

CARS spectra are recorded by measuring intensities of generated light at the anti-Stokes frequency $\omega_{AS} = 2\omega_1 - \omega_2$, integrated over the bandwidth $\Delta\omega_{AS}$ and as a function of the scanning frequency ω_2. The CARS spectra are calibrated on the ω_2-scale with an accuracy of 0.02 cm^{-1} by simultaneously recording an I_2-fluorescence spectrum with accurately calibrated lines [7]. Observed spectra for the three CARS processes are presented in figs. 3–5. Spectral features recorded with narrowband and broadband pump laser are related on the ω_2-frequency scale within 0.02 cm^{-1} by mapping corresponding calibration spectra.

3.1. Ground-state resonant CARS

In fig. 3 the spectra for the $v_a = 0$ to $v_c = 6$ Raman overtone in the electronic ground state $X\,^1\Sigma_g^+$ of I_2 are shown. The peaks in the spectra related to the resonance P(53), R(56), P(83) and P(103) of fig. 2 are denoted in the terminology for Raman transitions. From a comparison of the spectrum recorded with the broadband pump ($\Delta\omega_1 \approx 1$ cm^{-1}) and the narrowband ($\Delta\omega_1 \approx 0.005$ cm^{-1}) we find the following characteristics. The linewidths observed in the CARS spectra correspond to the bandwidth of the Stokes-laser and are independent of the bandwidth of the pump-laser. Within a margin of 0.05 cm^{-1} the resonance features appear at the same Stokes frequency, with the notable exception of Q(83) which is shifted by 0.6 cm^{-1} (see fig. 3). Moreover the relative intensities change somewhat with a marked increase in signal for the Q(83) line in the spectrum taken with the broadband pump.

For an interpretation of these phenomena we consider the appropriate energy level diagram of fig. 1, both for the situation of broadband and narrowband pumping. In case of a narrowband pump ω_1 the Raman resonances will be found at $\Delta\omega = \omega_1 - \omega_2 = \omega_{ca}$ (fig. 1a). The CARS signal is enhanced by the ω_{ba}-resonance, but because of the fixed and narrowband

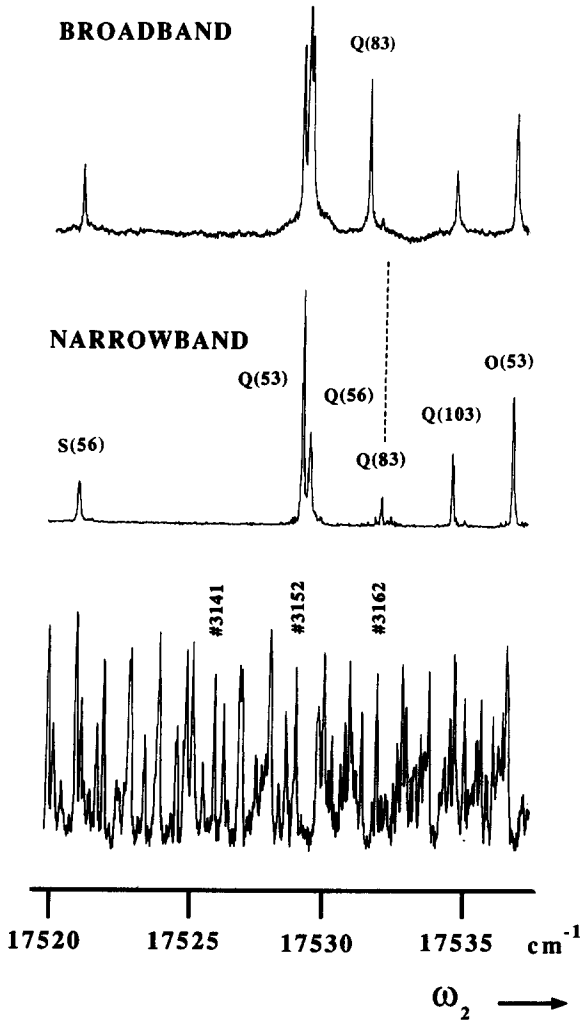

Fig. 3. Resonant ground-state CARS spectra of the $\Delta v=6$ Raman overtone in the electronic ground state $X\,^1\Sigma_g^+$ in I_2 taken with broadband ω_1 (upper spectrum) and narrowband ω_1 (middle spectrum). The reference I_2-fluorescence spectrum is simultaneously recorded (lower spectrum). A few lines are numbered according to he I_2-atlas [7].

frequency of ω_1 there will be a detuning at the one-photon resonance: $\delta\omega=\omega_1-\omega_{ba}$. This detuning is small (at most 0.1 cm^{-1}) for P(53), R(56) and P(103), but $\delta\omega$ for the P(83) resonance is about 0.6 cm^{-1} ($\omega_1\cong 18788.40(5)$ cm^{-1} for the recording in fig. 3). This is the reason that in narrowband pump excitation the Q(83) feature is weak. Its Raman resonance on the ω_2-scale is then expected at $\omega_2=\omega_1-\omega_{ca}=17532.04$ cm^{-1} ($\omega_{ca}=1256.36$ cm^{-1}) and this coincides with the weak line in the narrowband spectrum in fig. 3.

For a broadband pump the resonance conditions on the ω_2-scale, shown graphically in fig. 1b, are somewhat different. Certain frequency components within the profile $\Delta\omega_1$ will be in exact resonance with the transitions ω_{ba} that lie within the grey shaded area of fig. 2. In this case the Raman resonance condition will be fulfilled exactly for $\omega_2=\omega_{bc}$ independent of the width of the pump at ω_1. This explains why the CARS features in the upper spectrum of fig. 3 remain narrow, even with broadband pumping. A calculation of the transition $B\,^3\Pi_{u0}^+-X\,^1\Sigma_g^+$ (33, 6) P(83) now gives $\omega_2=\omega_{bc}=17531.45$ cm^{-1} exactly coinciding with the position of the Q(83) line in the broadband CARS spectrum of fig. 3. This explains the shift of 0.6 cm^{-1} in the position of Q(83) when comparing the two situations. For the other lines in the spectrum no shift is observed. For these lines the narrowband ω_1 is only slightly off-resonant and the resolution of the Stokes-laser is not sufficiently good to record small shifts. The relative intensities change when comparing the broadband and narrowband spectra. Especially the Q(83) line profits from the broadband pump source as frequency components from the ω_1-profile are now on resonance with P(83).

3.2. Excited-state parametric CARS

In fig. 4 the spectra corresponding to the $v_{b'}=32\leftrightarrow v_{d'}=53$ Raman resonance in the electronically excited state $B\,^3\Pi_{u0}^+$ in I_2 are shown. The most pronounced features in the spectra are due to the P(53) and R(56) (32, 0) one-photon resonance at the frequency ω_1. The lines are denoted by their Raman rotational transition in the excited electronic state. The effect of a change in the bandwidth of the ω_1-beam is striking. In the case where the narrowband ω_1 is used the CARS lines have a width (0.09 cm^{-1}) slightly larger than the bandwidth of the ω_2-dye-laser. With the broadband ω_1 the lines have a width of 1.1(1) cm^{-1}, which apparently equals the width of the pump laser. Furthermore, on the ω_2-scale the lines are shifted when comparing the two spectra.

For an interpretation of these effects we consider the energy level diagram of fig. 1, pertaining to the excited-state parametric CARS process. In case of a broadband pump again only the frequency compo-

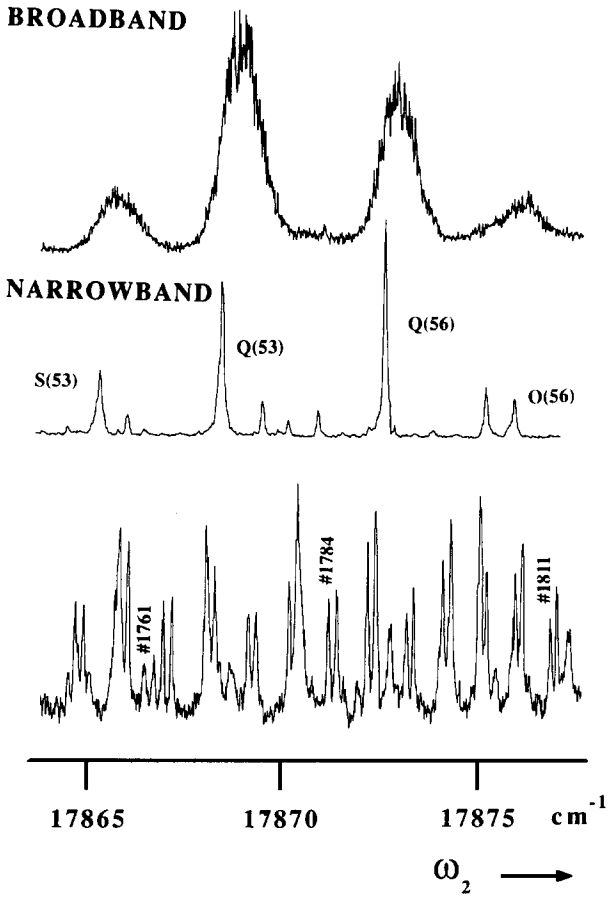

Fig. 4. Excited-state parametric CARS spectra of the $v=32 \leftrightarrow v=53$ Raman resonance in the electronic excited state $B\,^3\Pi_{u0}^+$ in I_2 taken with broadband ω_1 (upper spectrum) and narrowband ω_1 (middle spectrum). The reference I_2-fluorescence spectrum is simultaneously recorded (lower spectrum).

nents fitting to a $\omega_{b'a'}$ resonance in the first photon interaction give rise to enhancement. On a scale of ω_2, which is the tuned parameter in the observed spectrum, the Raman resonance condition is $\omega_2 = \omega_1 - \omega_{d'b'}$. Because of the broad continuum $|c'\rangle$ this resonance condition can be fulfilled for any frequency component ω_1 present in the pump laser. Indeed the width of ω_1 appears in the observed resonant CARS spectrum. From the line centres of the CARS features we determined a rather accurate value for the centre frequency of the unseeded Nd:YAG laser: 18788.39 ± 0.05 cm^{-1}.

In case of a narrowband pump excitation CARS resonances are expected whenever $2\omega_1 - \omega_2$ coincides with a resonance $\omega_{d'a'}$ (see fig. 1a). The first ω_1-photon gives rise to resonance-enhancement on the transition $a' \leftrightarrow b'$. The second resonance produces no selectivity because $2\omega_1$ is always in resonance with the continuum $|c'\rangle$. So in case of the narrowband ω_1 the only resonance condition is $\omega_{AS} = 2\omega_1 - \omega_2 = \omega_{d'a'}$, or in terms of the Stokes frequency: $\omega_2 = 2\omega_1 - \omega_{d'a'}$. From a calculation of energy level positions $|d'\rangle$ and $|a'\rangle$ for the resonances involved we find that the frequencies of observed features are in agreement with a value $\omega_1 = 18788.52 \pm 0.05$ cm^{-1}.

So in the CARS spectrum taken with the broadband pump the positions of the resonance features are determined by $\omega_2 = \omega_1 - \omega_{d'b'}$ and in the spectrum taken with the narrowband pump by $\omega_2 = 2\omega_1 - \omega_{d'a'}$. This also explains the observed shifts of 0.38(2) cm^{-1} in the Q(53) and S(53) lines, and of 0.23(2) cm^{-1} in the Q(56) line in the two spectra of fig. 4. To illustrate this phenomenon of resonance shifting the narrowband frequency was purposely tuned away from the centre of the profile of the broadband pump.

3.3. Excited-state non-parametric CARS

In fig. 5 the spectra corresponding to excited-state non-parametric CARS are shown. A Raman resonance between states $v_{b''} = 32$ and $v_{d''} = 16$ (or 17 for $J_{a''} = 103$) is probed in the excited electronic state $B\,^3\Pi_{u0}^+$ in I_2. Again the most pronounced features correspond to $J_{a''} = 53$, 56 and 103 determined by the one-photon resonance of the pump laser ω_1. The lines are again denoted in Raman terminology.

As in the case of ground-state resonant CARS no effect of the pump bandwidth $\Delta\omega_1$ is found in the spectral linewidths. In both cases the linewidths correspond to that of the Stokes-laser ω_2. For the observed features in the excited-state non-parametric process an explanation analogous to that presented for the ground-state resonant CARS process can be given. The interactions with the photons ω_1 and ω_2 are in resonance or in near resonance with the $B\,^3\Pi_{u0}^+ - X\,^1\Sigma_g^+$-system of I_2. In case of broadband pump-excitation again only frequency components that are in resonance with $\omega_{b''a''}$ are selected. The CARS features are found at $\omega_2 = \omega_{d''a''}$ on the ω_2-

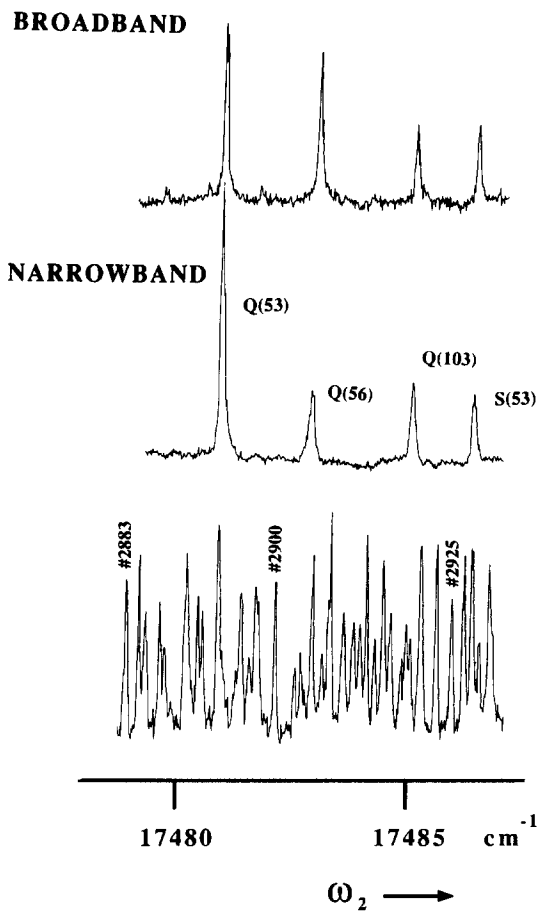

Fig. 5. Excited-state non-parametric CARS spectra of the $v=32 \leftrightarrow v=16(17)$ Raman resonance in the electronic excited state $B\,^3\Pi_{u0}^+$ in I_2 taken with broadband ω_1 (upper spectrum) and narrowband ω_1 (middle spectrum). The reference I_2-fluorescence spectrum is simultaneously recorded (lower spectrum).

scale. This agrees with calculations of transition frequencies in I_2. Moreover, the resonance condition $\omega_2=\omega_{d''a''}$ is independent of ω_1 and this explains why the features remain narrow even in broadband excitation.

4. Concluding remarks

In the present paper additional support is presented that confirms the identification of three different threefold-resonant four-wave mixing processes in I_2. The initial identification [1] was based on the spectral characteristics of the lines observed. The effect of the ω_1-laser bandwidth on the spectral linewidth and the slightly altered frequency position of the lines is yet another confirmation of the resonance schemes. In a more general sense it shows that linewidth effects may be used for identification of multiple resonance four-wave-mixing processes.

On the basis of the qualitative picture presented in this paper a prediction can be made concerning the bandwidth of the generated anti-Stokes wave. When the anti-Stokes resonance is a bound–bound transition the bandwidth is expected to reflect the width of this transition. Such will be the case for the excited-state parametric CARS process. In the ground-state resonant CARS process and the excited-state non-parametric CARS process and the anti-Stokes resonance is a continuum–bound transition and will therefore result in a bandwidth $\Delta\omega_{AS}$ which is determined by the bandwidth of the pump-laser.

References

[1] I. Aben, W. Ubachs, P. Levelt, G. v.d. Zwan and W. Hogervorst, Phys. Rev. A 44 (1991) 5881.
[2] B. Attal, O.O. Schnepp and J.-P. Taran, Optics Comm. 24 (1978) 77.
[3] A. Beckman, H. Fietz, P. Baierl and W. Kiefer, Chem. Phys. Lett. 86 (1982) 140.
[4] C.S. Dimov, L.I. Pavlov, K.V. Stamenov and K.V. Khadzhiisky, J. Raman Spectrosc. 17 (1986) 277.
[5] P. Luc, J. Molec. Spectrosc. 80 (1980) 41.
[6] I. Aben, W. Ubachs, G. v.d. Zwan and W. Hogervorst, Mol. Phys. 76 (1992) 591.
[7] S. Gerstenkorn and P. Luc, Atlas du Spectre d'Absorption de la Molecule d'Iode (Editions du CNRS, Paris, 1977).